Intramolecular Photoinduced Charge Separation and Charge Recombination of the Product Ion Pair States of a Series of Fixed-Distance Dyads of Porphyrins and Quinones: Energy Gap and Temperature Dependences of the Rate Constants

Tsuyoshi Asahi,[†,§] Masaya Ohkohchi,[†] Ryohzi Matsusaka,[†] Noboru Mataga,*[,†] Run Ping Zhang,[‡] Atsuhiro Osuka,*[,‡] and Kazuhiro Maruyama[‡]

Contribution from the Department of Chemistry, Faculty of Engineering Science, Osaka University, Toyonaka, Osaka 560, Japan, and Department of Chemistry, Faculty of Science, Kyoto University, Kyoto 606, Japan

Received September 3, 1992

Abstract: Intramolecular photoinduced charge separation (CS) and charge recombination (CR) of the product ion pair (IP) state of a series of fixed-distance dyads consisting of free-base porphyrin or zinc porphyrin and quinones have been investigated by means of picosecond–femtosecond laser spectroscopies in order to examine the energy gap and temperature dependences of CS and CR reactions in nonpolar media. Obtained CS rates were in the normal region, up to the neighborhood of the top region, and CR rates were in the inverted region; their energy gap dependences at room temperature were approximately reproduced by a semiclassical formula taking into consideration the high-frequency quantum mode of nuclear vibrations, although the CS rates near the top region did not show indication of the shift to the inverted region, contrary to the calculation. We have confirmed that the activation barrier for the CS reaction increases with a decrease of the energy gap, while the CR process is activationless, indicating the dominant effect of the high-frequency quantum mode in the inverted region. However, we could hardly find optimum parameter values for reorganization energies, etc., in the theoretical equation which could reproduce quantitatively both the energy gap dependence and the temperature dependence of the CS and CR rates at the same time. We have examined also the solvent polarity effect upon the energy gap ($-\Delta G_{CS}$) dependence of the CS rate constant (k_{CS}) which showed a rather large systematic change corresponding to the increase of the solvent reorganization energy with the increase of the solvent polarity, while the energy gap ($-\Delta G_{CR}$) dependence of the CR rate constant (k_{CR}) showed little solvent polarity dependence, leading to the crossing between the k_{CS} vs $-\Delta G_{CS}$ curve in the normal to near the top region and the k_{CR} vs $-\Delta G_{CR}$ in the inverted to near the top region. Implications of these results, which seem difficult to interpret on the basis of the conventional electron-transfer theories, are discussed on the basis of the dominant effect of the quantum mechanical tunneling in the inverted region and/or the existence of nonlinear or some specific interactions between the IP state and the surrounding polar solvent.

The mechanisms and dynamics of photoinduced electron transfer (ET), such as the charge separation (CS) and the charge recombination (CR) of the product ion pair (IP) state as well as the charge shift (CSH) reaction in the condensed phase, are the most fundamental and important problems in chemistry and biology.[1-6] The ET reaction rates are regulated by various factors, including the magnitude of the electronic coupling responsible for ET between electron donor (D) and electron acceptor (A) (which depends also on their mutual distance and orientation), the free energy gap between the initial and final states (the reaction exothermicity, $-\Delta G$), the orientation of the solvent surrounding D and A, and the temperature.

In many cases, ET takes place by very weak electronic coupling between D and A, where the nonadiabatic approximation is valid and the ET rate constant k_{et} is given by

$$k_{et} = (2\pi/\hbar)V^2\mathrm{FCWD} \qquad (1)$$

where V is the electronic coupling and FCWD represents the Franck–Condon weighted density of states. FCWD depends on the energy gap, $-\Delta G$, and nuclear vibrational modes relevant to the ET process, the differences of bond lengths and bond angles, and the orientations of surrounding media (solvents) between the initial and final states. The temperature effect on the reaction rate is believed to originate mainly from the temperature dependence of FCWD.

The usual theoretical treatment of ET reactions as represented by eq 1 predicts a bell-shaped energy gap dependence, i.e., the increase of k_{et} with the energy gap at first (normal region) and the decrease of k_{et} with a further increase of energy gap (inverted region). However, only the normal and the top region have been observed, and the existence of the inverted region has not been confirmed up to now in the experimental investigations of photoinduced CS reactions.[6b,c,7,8] On the other hand, the theoretically expected bell-shaped energy gap dependence, including both the inverted region and the normal region, has been

† Osaka University.
‡ Kyoto University.
§ Present address: Department of Applied Physics, Osaka University, Suita, Osaka 565, Japan.

(1) (a) Mataga, N.; Ottolenghi, M. In *Molecular Association*; Foster, R., Ed.; Academic: New York, 1979; Vol. 2, p 1. (b) Mataga, N. *Pure Appl. Chem.* **1984**, *56*, 1255.
(2) Marcus, R. A.; Sutin, N. *Biochem. Biophys. Acta* **1985**, *811*, 265.
(3) Rips, I.; Klafter, J.; Jortner, J. In *Photochemical Energy Conversion*; Norris, J. R., Meisel, D., Eds.; Elsevier: New York, 1988; p 1.
(4) Maroncelli, M.; McInnis, J.; Fleming, G. R. *Science* **1989**, *243*, 1674.
(5) Barabara, P. F.; Jarzeba, W. *Adv. Photochem.* **1990**, *15*, 1.
(6) Some other reviews of recent developments: (a) *Perspectives in Photosynthesis*; Jortner, J., Pullman, B., Eds.; Kluwer Academic: Dordrecht, 1990. (b) *Electron Transfer in Inorganic, Organic and Biological Systems*; Bolton, J. R., Mataga, N., McLendon, G., Eds.; Advances in Chemistry Series 228; American Chemical Society: Washington, DC, 1991. (c) *Dynamics and Mechanisms of Photoinduced Electron Transfer and Related Phenomena*; Mataga, N., Okada, T., Masuhara, H., Eds.; Elsevier: Amsterdam, 1992. (d) Verhoeven, J. W. *Pure Appl. Chem.* **1990**, *62*, 1585.
(7) Rehm, D.; Weller, A. *Isr. J. Chem.* **1970**, *7*, 259.
(8) (a) Mataga, N.; Kanda, Y.; Asahi, T.; Miyasaka, H.; Okada, T.; Kakitani, T. *Chem. Phys.* **1988**, *127*, 239. (b) Nishikawa, S.; Asahi, T.; Okada, T.; Mataga, N.; Kakitani, T. *Chem. Phys. Lett.* **1991**, *185*, 237.

0002-7863/93/1515-5665$04.00/0

observed in the case of the CR reaction of geminate IP produced by the photoinduced CS reaction between the fluorescer and quencher in acetonitrile solution.[9,10]

In order to give a reasonable interpretation of the apparent lack of the inverted region in the photoinduced CS reaction and/or of the remarkable difference between the energy gap dependence of CS and CR reactions, several possibilities (such as the participation of the excited electronic states of IP[7,8,11] and/or the formation of a nonfluorescent charge-transfer complex[8] in the course of quenching and the nonlinear polarization of the solvent around the charged solute[12]) were proposed. For a more quantitative treatment of this problem, however, we have demonstrated recently that it is necessary to take into account the distribution of the D–A distance in the CS process[13] and some relaxation of this distribution in the course of CR in addition to a moderate nonlinear polarization of the solvent around the charged solute. Moreover, such distance distribution producing the different kinds of geminate IPs depending on the $-\Delta G$ values of CS seems to play generally important roles in determining the mechanisms of chemical reactions caused by photoinduced ET.[8b,13,14]

Nevertheless, for an unambiguous experimental confirmation of such theoretical considerations (including the effects of the D–A distance distribution, solvent polarization, etc., on the energy gap dependence of the ET reaction), investigations on the photoinduced CS and the CR of geminate IP of fixed-distance-linked D–A systems with various $-\Delta G$ values for CS and CR will be of crucial importance. Systematic studies of the temperature effects on the photoinduced CS and CR of the product IP state will be possible also by using such fixed-distance linked D–A systems. Otherwise a larger freedom of motion of the components will obscure the results of the measurements. Although there were many investigations on the energy gap dependence of the ET rate, only a few such systematic studies on the fixed-distance systems were available,[15,16] and there remain many problems to be elucidated. In this respect, we have undertaken a detailed picosecond–femtosecond laser photolysis investigation of the energy gap as well as the temperature dependence of the photoinduced CS and CR of the product IP state of a series of fixed-distance porphyrin–quinone dyads (Figure 1) in such nonpolar or only slightly polar solvents as benzene and toluene. We have examined also the effects of the solvent polarity on the energy gap dependence of these ET processes by investigating the same dyads in polar solvents such as tetrahydrofurane (THF) and butyronitrile (BuCN) and by comparing the results with those from the benzene solutions. These are the first systematic experimental findings on the solvent polarity effect on the energy gap dependences of both photoinduced CS and CR of the IP state determined by using fixed-distance D–A dyads of organic chromophores.

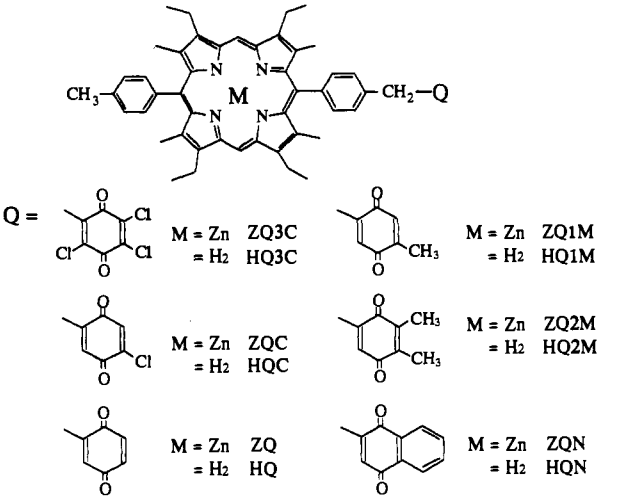

Figure 1. Structural formulas of the P–Q compounds.

It should be noted here that some systematic investigations concerning the solvent polarity and temperature effects on k_{CS} of D–A-linked systems were reported recently,[17-21] the results of which were in accord with the conventional ET theory. In the present work, however, we are concerned with a more direct experimental observation of k_{CS} vs $-\Delta G_{CS}$ and k_{CR} vs $-\Delta G_{CR}$ relations in the case of fixed-distance dyads of porphyrin–quinone and have investigated solvent polarity effects on these energy gap dependences of k_{CS} and k_{CR}.

Usually, in the analysis of the experimental results, the following simplified equation (eq 2) derived by assuming that the relevant high-frequency vibrations can be replaced by one mode with an averaged angular frequency,[2,20,21] is frequently used:

$$k_{et} = (\pi/\hbar^2\lambda_s k_B T)^{1/2} V^2 \sum_n (e^{-S}(S^n/n!)) \times \exp\{-(\Delta G + \lambda_s + n\hbar\langle\omega\rangle)^2/4\lambda_s k_B T\} \quad (2)$$

where $S = \lambda_v/\hbar\langle\omega\rangle$ is the coupling constant, λ_v is the reorganization energy associated with the averaged angular frequency $\langle\omega\rangle$, and λ_s is the solvent reorganization energy treated classically. Although this sort of equation is rather widely used and we shall also use such an equation in the present work, it should be noted here that the validity of this sort of approximate equation is not necessarily warranted in the quantitative analyses of the experimental results. We shall also examine this question in the following sections.

Experimental Section

The details on the syntheses of the P–Q compounds (Figure 1) will be described elsewhere.[22] The compounds were purified by repetitive TLC and recrystallization. Benzene and toluene were spectrograde (Merck Uvasol) and were passed through a column of silica gel several times before use. Spectrograde (Merck Uvasol) THF was passed through molecular sieves several times before use. BuCN (Wako G.R. grade) was dried by being passed over molecular sieves and calcium hydride and

(9) (a) Mataga, N.; Asahi, T.; Kanda, Y.; Okada, T.; Kakitani, T. *Chem. Phys.* **1988**, *127*, 249. (b) Ohno, T.; Yoshimura, A.; Mataga, N. *J. Phys. Chem.* **1986**, *90*, 3295. (c) Mataga, N.; Kanda, Y.; Okada, T. *J. Phys. Chem.* **1986**, *90*, 3880.

(10) (a) Gould, I. R.; Ege, D.; Mattes, S. L.; Farid, S. *J. Am. Chem. Soc.* **1987**, *109*, 3794. (b) Gould, I. R.; Ege, D.; Moser, J. E.; Farid, S. *J. Am. Chem. Soc.* **1990**, *112*, 4290.

(11) Mataga, N. *Bull. Chem. Soc. Jpn.* **1970**, *43*, 3623.

(12) (a) Kakitani, T.; Mataga, N. *J. Phys. Chem.* **1985**, *89*, 8. (b) Yoshimori, A.; Kakitani, T.; Enomoto, Y.; Mataga, N. *J. Phys. Chem.* **1989**, *93*, 8316.

(13) Kakitani, T.; Yoshimori, A.; Mataga, N. *J. Phys. Chem.* **1992**, *96*, 5385.

(14) Miyasaka, H.; Morita, K.; Kamada, K.; Nagata, T.; Kiri, M.; Mataga, N. *Bull. Chem. Soc. Jpn.* **1991**, *64*, 3229.

(15) Miller, J. R.; Calcaterra, L. T.; Closs, G. L. *J. Am. Chem. Soc.* **1984**, *106*, 2047.

(16) (a) Wasielewski, M. R. In *Photoinduced Electron Transfer, Part A*; Fox, M. A., Chanon, M., Eds.; Elsevier: Amsterdam, 1988; Chapter 1.4. (b) Wasielewski, M. R.; Gaines, G. L., III; O'Neil, M. P.; Svec, W. A.; Niemczyk, M. P.; Prodi, L.; Gosztola, D. In *Dynamics and Mechanisms of Photoinduced Electron Transfer and Related Phenomena*; Mataga, N., Okada, T., Masuhara, H., Eds.; Elsevier: Amsterdam, 1992; p 87. (c) Gaines, G. L., III; O'Neil, M. P.; Svec, W. A.; Niemczyk, M. P.; Wasielewski, M. R. *J. Am. Chem. Soc.* **1991**, *113*, 719.

(17) (a) Bolton, J. R.; Schmidt, J. A.; Ho, T.-F.; Liu, J.-Y.; Roach, K. J.; Weeden, A. C.; Archer, M. D.; Wilford, J. H.; Gadzekpo, V. P. Y. In *Electron Transfer in Inorganic, Organic and Biological Systems*; Bolton, J. R., Mataga, N., McLendon, G. L., Eds.; Advances in Chemistry Series 228; American Chemical Society: Washington, DC, 1991; Chapter 7, p 177. (b) Liu, J.-Y.; Bolton, J. R. *J. Phys. Chem.* **1992**, *96*, 1718. (c) Liu, J.-H.; Schmidt, J. A.; Bolton, J. R. *J. Phys. Chem.* **1991**, *95*, 6924. (d) Schmidt, J. A.; Liu, J.-Y.; Bolton, J. A.; Archer, M. D.; Gadzekpo, V. P. Y. *J. Chem. Soc., Faraday Trans. 1* **1989**, *85*, 1027.

(18) Kroon, J.; Verhoeven, J. W.; Paddon-Row, M. N.; Oliver, A. M. *Angew. Chem.* **1991**, *30*, 1358.

(19) Heitele, H.; Pollinger, F.; Kremer, K.; Michel-Beyerl, M. E.; Futscher, M.; Voit, G.; Weiser, J.; Staab, H. A. *Chem. Phys. Lett.* **1992**, *188*, 270.

(20) Jortner, J. *J. Chem. Phys.* **1976**, *64*, 4860.

(21) Miller, J. R.; Beitz, J. V.; Huddleston, R. K. *J. Am. Chem. Soc.* **1984**, *106*, 5057.

(22) Osuka, A.; Zhang, R. R.; Maruyama, K.; Yamazaki, I.; Nisimura, Y. *Bull. Chem. Soc. Jpn.* **1992**, *65*, 2807.

Table I. Observed Fluorescence Lifetimes (τ_s) of P–Q Compounds in Benzene Solutions and CS Rate Constants (k_{CS}) Obtained from the τ_s Values

	τ_s (ps)[a]	k_{CS} (10^{10} s^{-1})
ZQ3C		
ZQC		
ZQ	3.7 (0.994)	27.0
ZQ1M	13.4 (0.903)	7.4
ZQ2M	17.4 (0.993)	5.7
ZQN	12.9 (0.980)	7.7
HQ3C		
HQC		
HQ	51.6 (0.996)	1.9
HQ1M	125 (0.919)	0.79
HQN[b]	109 (0.407)	0.42
	1200 (0.564)	

[a] Values in parentheses are the fractions of the fluorescence yield of P–Q compounds in the total fluorescence including that of the impurity with reduced quinone (see text). [b] Fluorescence decay curve of HQN shows double exponential decay due to the back-ET to the fluorescence state from the intramolecular IP state (see text).

distilled several times before use. The solutions for measurement were deoxygenated by purging with nitrogen gas, and their concentrations were 10^{-6} M for the measurement of fluorescence lifetime and fluorescence spectra and 10^{-4} M for time-resolved transient absorbance spectral measurements.

Fluorescence decay curves were measured by means of a time-correlated single photon counting method using a synchronously pumped cavity-dumped dye laser with the second harmonic of pyridine-1 (355 nm) as an excitation source.[8b] The observation was made at the peak wavelength of the fluorescence band (635 nm for the free-base porphyrin and 585 nm for the zinc porphyrin). SALS at the Osaka University Computation Center was used for the nonlinear least-squares analysis of the observed decay curves.

Picosecond time-resolved transient absorption spectral measurements were performed as described previously using a microcomputer-controlled picosecond laser photolysis system with a mode-locked Nd^{3+}:YAG laser (fwhm = 24 ps at fundamental).[23] Second harmonic generation (SHG) was used for exciting sample solutions. A microcomputer-controlled femtosecond laser photolysis system was used for the measurement of time-resolved transient absorption spectra in the 100-fs to 10-ps time region.[24] The SHG (355 nm) pulse of the pyridine-1 dye laser was used for exciting the samples.

Cyclic voltametry was performed with a PAR Model 174 in CH_2Cl_2 containing tetra-*n*-butylammonium perchlorate at room temperature and using a Pt electrode.

Results and Discussion

(A) Photoinduced Electron Transfer in Benzene Solutions at Room Temperature (22 ± 1 °C). Ground-state absorption spectra and fluorescence spectra of the P–Q compounds were practically identical to those of the reference compounds without attached quinone. Fluorescence yields and lifetimes, however, were extremely decreased compared with those of the corresponding reference compounds. Observed fluorescence decay curves were biphasic and reproduced with the double exponential decay function, except for the case of HQN. The decay time of the long-lived component did not depend on the nature of the appended quinones and was the same as that of the reference porphyrin. Therefore, the long-lived component can be ascribed to the impure compound, where the porphyrin is linked with reduced quinone, while the short-lived one is due to the decay of $P^*(S_1)$–Q. The fraction of the former in the total fluorescence was estimated to be less than several percent from the preexponential factor in the fluorescence decay function (see Table I). The extremely short decay time τ_s of $P^*(S_1)$–Q (compared with the decay time τ_0 of the reference porphyrin)[25] as shown in Table I can be ascribed entirely to intramolecular ET. We have actually confirmed ET-state formation by time-resolved transient absorption spectral measurements. The k_{CS} values indicated in Table I were obtained by $k_{CS} = \tau_s^{-1} - \tau_0^{-1}$.

In the case of HQN, it was not possible to reproduce the fluorescence decay curve by the double exponential formula, but three exponential formulas were necessary, where one component is due to the small amount of the impurity with reduced quinone. This means that the decay of the S_1 state of HQN in benzene is intrinsically biphasic, which may be due to the thermal repopulation of the S_1 state from the IP state, P^+–Q^-. As is discussed later in detail, we have observed similar behaviors of HQN also by the transient absorption spectral measurements.

As an example of the time-resolved transient absorption spectra, results of HQ observed by exciting the solution with a picosecond 532-nm laser pulse are indicated in Figure 2A. Immediately after excitation, mainly the $S_1 - S_0$ difference spectrum, characterized by the bleaching of the ground-state porphyrin absorption at 505 and 575 nm of the Q-band, and a strong positive absorbance with its maximum near 445 nm are observed. Along with the rapid decay of the 445-nm band, new broad bands with maxima at 700 and 460 nm due to the porphyrin cation (P^+) and the quinone anion (Q^-)[26] arise. The spectrum at 1-ns after excitation can be ascribed to the S_1 and/or the T_1 state of

Table II. Values of ϵ_{S1}, ϵ_{ion},[a] and $\epsilon_{T1}\Phi_T$ (L mol^{-1} cm^{-1}) Used for the Analysis of the Transient Absorption Spectra In Benzene and Toluene Solutions

In Benzene and Toluene Solutions

	ZnP–Q		H_2P–Q	
	460 nm	650 nm	445 nm	700 nm
ϵ_{S1}	4.9×10^4	0.3×10^4	3.0×10^4	0
ϵ_{ion}	1.4×10^4	1.3×10^4 [b]	1.3×10^4	1.2×10^4
$\epsilon_{T1}\Phi_T$	4.8×10^4	0.3×10^4	3.5×10^4	0.35×10^4

In THF and BuCN Solutions

	ZnP–Q	
	460 nm	650 nm
ϵ_{S1}	6.0×10^4	0.4×10^4
ϵ_{ion}	1.4×10^4	1.0×10^4
$\epsilon_{T1}\Phi_T$	6.0×10^4	0.4×10^4

[a] Sum of the absorption coefficients of porphyrin cation and quinone anion. [b] 1.4×10^4 was used for ZQN because the difference absorption of 1,4-naphthoquinone anion at this wavelength is different from that of the other quinone anions.[26]

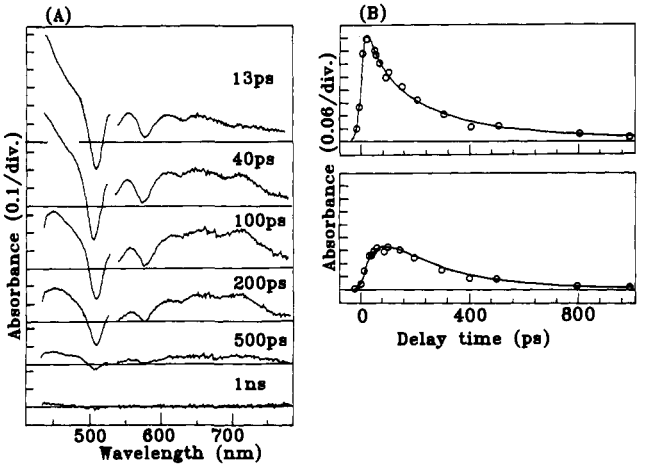

Figure 2. (A) Time-resolved transient absorption spectra of HQ in benzene observed by excitation with a 532-nm picosecond pulse. (B) Time profiles of absorbance of HQ in benzene at 445 (top) and 700 nm (bottom). The solid lines are the simulated curves by convolution of exciting pulse, transient absorption (eq 3), and probing pulse, with τ_s = 45 ps and τ_{ion} = 240 ps.

(23) Miyasaka, H.; Masuhara, H.; Mataga, N. *Laser Chem.* **1983**, *1*, 357.
(24) (a) Mataga, N.; Miyasaka, H.; Asahi, T.; Ojima, S.; Okada, T. *Ultrafast Phenomena VI*; Springer-Verlag: Berlin, 1988; p 511. (b) Miyasaka, H.; Ojima, S.; Mataga, N. *J. Phys. Chem.* **1989**, *93*, 3380.
(25) The fluorescence lifetimes τ_0 of reference porphyrins are 1.3 (zinc porphyrin) and 12.4 ns (free-base porphyrin) in toluene solutions.
(26) Shida, T. *Electronic Absorption Spectra of Radical Ions*; Elsevier: Amsterdam, 1988.

Table III. Lifetimes of $P^*(S_1)$–Q (τ_S) and P^+–Q^- (τ_{ion}) States, CS Rate Constants (k_{CS}), CR Rate Constants (k_{CR}), and Free Energy Gaps for CS Reaction ($-\Delta G_{CS}$) and CR Reaction ($-\Delta G_{CR}$) in Benzene Solutions Obtained by Transient Absorption Spectroscopy

	τ_s (ps)	k_{CS} (10^{10} s^{-1})	$-\Delta G_{CS}$ (eV)	τ_{ion} (ps)	k_{CR} (10^{10} s^{-1})	$-\Delta G_{CR}$ (eV)
ZQ3C	2.5	40	0.95	12	9.7	1.18
ZQC	5.6	18	0.72	40	2.5	1.41
ZQ	6.2	16	0.54	140	0.71	1.59
ZQ1M	10.5	9.5	0.46	240	0.42	1.67
ZQ2M	16	6.0	0.39	440	0.23	1.74
ZQN	14	7.0	0.36	400	0.25	1.77
HQ3C	3.0	33	0.59	13	7.7	1.38
HQC	15	6.7	0.36	70	1.4	1.61
HQ	45	2.1	0.18	240	0.42	1.79
HQ1M	120	0.78	0.10	330	0.30	1.87
HQN	109	0.42	0	1200	0.18	1.97
	1200					

porphyrin, mainly due to the impurity within the reduced quinone. The above results in Figure 2A show clearly that the quenching of the S_1 state of porphyrin in HQ results in the formation of the intramolecular IP state which disappears by the CR reaction to the ground state. Similar temporal changes of transient absorption spectra due to the photoinduced CS and CR of the product IP state have been observed also in other P–Q compounds.

In Figure 2B, we show time profiles of transient absorbances at 445 and 700 nm, which are the wavelengths of the absorption maxima of the S_1 and P^+ states, respectively. We have examined these experimental results on the basis of the following simple reaction scheme.

Scheme I

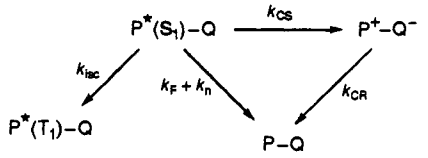

The time profile of the transient absorbance at a wavelength ($A_\lambda(t)$) is given as follows:

$$A_\lambda(t) = A_0\{\epsilon_{S_1} - \epsilon_{ion}\Phi_{ET}\tau_s^{-1}/(\tau_s^{-1} - \tau_{ion}^{-1}) - \epsilon_{T_1}\Phi_T(1 - \Phi_{ET})\}\exp(-t/\tau_s) + A_0\{\epsilon_{ion}\Phi_{ET}\tau_s^{-1}/(\tau_s^{-1} - \tau_{ion}^{-1})\}\exp(-t/\tau_{ion}) + A_0\epsilon_{T_1}\Phi_T(1 - \Phi_{ET}) + A_0\Phi_0\{(\epsilon_{S_1} - \epsilon_{T_1}\Phi_T)\exp(-t/\tau_0) + \epsilon_{T_1}\Phi_T\} \quad (3)$$

where A_0 is the initial concentration of $P^*(S_1)$–Q, $\tau_s^{-1} = k_{CS} + \tau_0^{-1}$, $\tau_0^{-1} = k_{isc} + k_f + k_n$, $\tau_{ion}^{-1} = k_{CR}$, $\Phi_{ET} = k_{CS}\tau_s^{-1}$, $\Phi_T = k_{isc}\tau_0^{-1}$, and ϵ_{S_1}, ϵ_{T_1}, and ϵ_{ion} are the difference absorption coefficients of the S_1 state, the T_1 state, and the IP state at the wavelength, respectively. The last term in eq 3 is the correction for the absorption by the S_1 and/or the T_1 state with relative yield Φ_0 of the porphyrin due to a small amount of impurity within the reduced quinone. The effect of this term is negligibly small, and it is approximately time-independent because ϵ_{S_1} and $\epsilon_{T_1}\Phi_T$ are almost the same at the wavelength of the observation. In order to examine the time profiles of the observed transient absorbance on the basis of the Scheme I, we have compared the result of convolution of $A_\lambda(t)$ in eq 3 with the excitation pulse and the probe pulse to the observed result. The solid lines in Figure 2B are simulations of the observed data by the convolution, taking τ_s = 45 ps and τ_{ion} = 240 ps. The agreement between the experimental and calculated results is reasonably good. By similar analysis, we have determined τ_s and τ_{ion} values of the H_2P–Q compounds except for HQN, from which k_{CS} and k_{CR} values have been obtained as indicated in Table III.

In Figure 3, we show the results of ZQ2M as an example of ZnP–Q compounds. In this case, we have monitored time profiles of absorbance at 460 and 650 nm. These wavelengths correspond

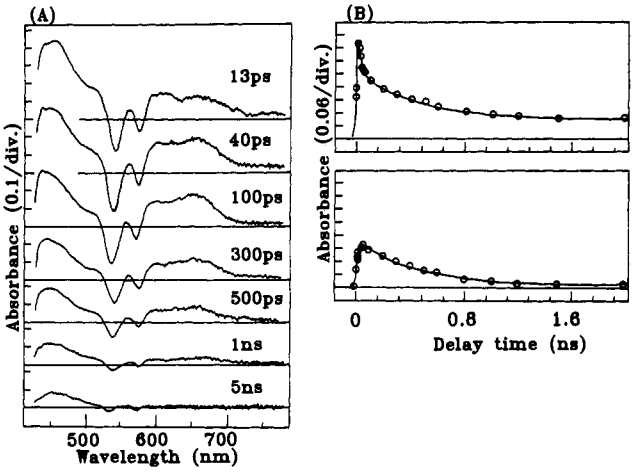

Figure 3. (A) Time-resolved transient absorption spectra of ZQ2M in benzene observed by excitation with a 532-nm picosecond pulse. (B) Time profiles of absorbance of HQ in benzene at 465 (top) and 650 nm (bottom). The solid lines are the simulated curves by convolution of exciting pulse, transient absorption (eq 3), and probing pulse, with τ_s = 16 ps and τ_{ion} = 440 ps.

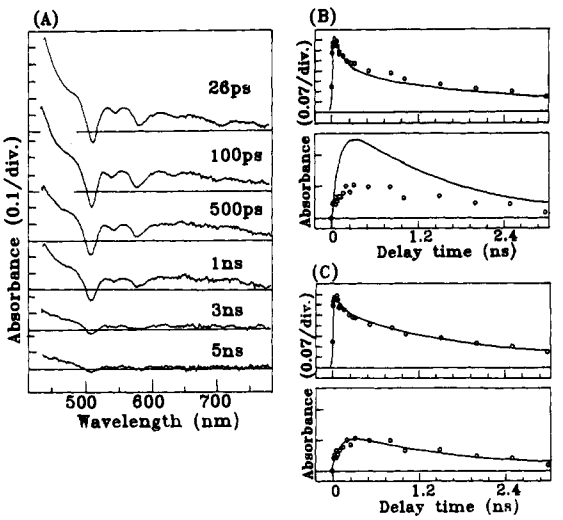

Figure 4. (A) Time-resolved transient absorption spectra of HQN in benzene observed by excitation with a 532-nm picosecond pulse. (B and C) Time profiles of absorbance of HQ in benzene at 445 (top) and 700 nm (bottom). The solid lines in spectrum B are the simulated curves based on Scheme I, and those of spectrum C are based on Scheme II (see text).

to the transient absorption spectrum of the S_1 state (460 nm) and that of the cation (650 nm), respectively. The simulated curves by the convolution in this case have been calculated with τ_s = 16 ps and τ_{ion} = 440 ps. We have determined by similar procedures τ_s and τ_{ion} values for other ZnP–Q compounds from which k_{CS} and k_{CR} values have been obtained as shown in Table III.

Actually, we have determined those τ_s and τ_{ion} values in such a way that the time profiles at the two wavelengths (445 and 700 nm for H_2P–Q; 460 and 650 nm for ZnP–Q) are consistent with each other by using the same values of ϵ_{S_1}, $\epsilon_{T_1}\Phi_T$, and ϵ_{ion} throughout the ZnP–Q compounds or H_2P–Q compounds. Those values of the extinction coefficients have been determined by means of measurements of transient absorbance and ground-state bleaching as well as of their excitation intensity dependence and are collected in Table II.

The time-resolved transient absorption spectra and time profiles of transient absorbance of HQN in benzene are indicated in Figure 4. As we have described already, the fluorescence decay of HQN is biphasic, which suggests the repopulation of the S_1 state of porphyrin by the return ET from the IP state. This is not unreasonable because the energy of the IP state of HQN is the highest and, accordingly, the closest to that of the porphyrin S_1

state among the compounds examined here. Actually, the time profiles of the transient absorbance cannot be reproduced by the simulation based on Scheme I as indicated in Figure 4B. In view of this we assume the following scheme for HQN.

Scheme II

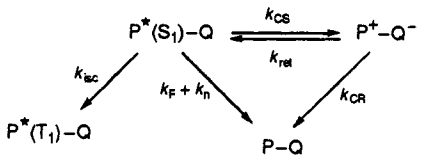

From this scheme, the decay function of the relative fluorescence intensity is given by

$$I_f(t) = C_1 \exp(-\mu_1 t) + C_2 \exp(-\mu_2 t)$$

$$\mu_{1,2} = {}^1/_2[\tau_0^{-1} + k_{CS} + k_{ret} + k_{CR} \mp \{(k_{ret} + k_{CR} - \tau_0^{-1} - k_{CS})^2 + 4k_{CS}k_{ret}\}^{1/2}]$$

$$C_1 = (\tau_0^{-1} + k_{CS} - \mu_2)/(\mu_1 - \mu_2)$$

$$C_2 = (\mu_1 - \tau_0^{-1} - k_{CS})/(\mu_1 - \mu_2) \quad (4)$$

The observed fluorescence decay curve can be reproduced satisfactorily by eq 4, from which we have obtained the following values of ET rate constants: $k_{CS} = 4.2 \times 10^9$ s^{-1}, $k_{CR} = 1.8 \times 10^9$ s^{-1}, and $k_{ret} = 4.0 \times 10^9$ s^{-1}. By using these rate constants and the values of the extinction coefficients given in Table II, we have simulated the time profiles of the transient absorbance as indicated in Figure 4C. The agreement between the calculated and observed results appears to be reasonably good. The k_{CS} and k_{CR} values of HQN in benzene obtained above are collected in Table III together with those of the other compounds examined in this work.

At this point, we should make some remarks on the possibilities of the effects of rotations of chromophore groups on the ET rate. Although the center-to-center P–Q distance is fixed, hindered rotations around the phenyl-CH_2 and/or CH_2-quinone bonds might be possible, leading to the rotational-angle-dependent ET or the formation of rotational conformers with different ET rates. If there exist such conformers and rotational motions in the excited state are sufficiently slower than the ET rate, then the decay curves of P*(S_1)–Q will be multiexponential. If the ET rate is rotational-angle-dependent and velocity of the rotational motion in the excited state is comparable with the ET rate, then the decay curve will become a complex nonexponential one. The decay curves of P*(S_1)–Q as well as the P^+–Q^- state observed by transient absorption measurements in benzene and toluene solutions were single exponential. We measured also the fluorescence decay curves of P*(S_1)–Q by the time-correlated single photon counting method with a picosecond dye laser as an excitation source for most of the systems. The decay curves were single exponential also by these measurements, with much higher dynamic range than the transient absorption measurements. These results indicate that no stable rotational isomer with different ET rate exists and/or that the rotational motion causing the change of ET rate is considerably slower than the ET. They suggest also that the conformation change by rotation may not affect so much the ET rate in these dyads. It is well-known that the conformation changes by internal rotation around the carbon–carbon single bond in some intramolecular exciplex systems are rather slow, with a time constant of ca. 1 ns,[1,27] which is considerably longer than most of the τ_s and τ_{ion} values of the dyads studied here. On the other hand, small torsional oscillations in the hindered rotational potential will be fast. However such oscillations may not affect the ET rate so much. The above results and arguments suggest that the intramolecular rotation may not affect the CS and CR rates in these dyads.

Table IV. Energies of the 0–0 Transitions between S_1 and S_0 States of P–Q Compounds in Benzene, THF, and BuCN Solutions (top) and Oxidation Potentials of Porphyrins (E_{ox}) and Reduction Potentials of Quinones (E_{red}) of P–Q Compounds (vs Ferrocene/Ferrocenium in CH_2Cl_2) (bottom)

	$\Delta E(S_1)$ (eV)		
solvent	benzene	THF	BuCN
ZnP–Q	2.13	2.13	2.15
H_2P–Q	1.97	1.98	1.97

	E_{ox} (eV)		E_{red} (eV)
ZnP–Q	0.13	Q3C	–0.65
H_2P–Q	0.33	QC	–0.88
		Q	–1.06
		Q1M	–1.14
		Q2M	–1.21
		QN	–1.24

(B) Free Energy Gap Dependence of k_{CS} and k_{CR} in Benzene Solutions at Room Temperature. We examine here the $-\Delta G$ dependence of k_{CS} and k_{CR} of the P–Q compounds with a fixed-distance D–A pair. For this purpose, we must determine the free energy gaps for the photoinduced CS ($-\Delta G_{CS}$) and those for the CR of the product intramolecular IP states ($-\Delta G_{CR}$) of these compounds in benzene solution.

Evidently, the following relations are valid for these $-\Delta G$s:

$$-\Delta G_{CS} = \Delta E(S_1) + \Delta G_{CR} \quad (5a)$$

$$-\Delta G_{CR} = E_{ox} - E_{red} + \Delta G_s \quad (5b)$$

where $\Delta E(S_1)$ is the energy of the 0–0 transition between the S_1 and the S_0 state of porphyrin, E_{ox} and E_{red} are respectively the half-wave potentials of one-electron oxidation of porphyrins and one-electron reduction of quinones in CH_2Cl_2 solutions (as given in Table IV), and ΔG_s is the correction term for the effects of the solvent polarity as well as the Coulombic energy between the charged donor and acceptor. In this work, we have determined the values of ΔG_s in benzene solution by using only the experimental data and without resorting to any correction formula. From the analysis of the time-resolved fluorescence and transient absorption measurements, k_{CS} and k_{ret} of HQN have been confirmed to be very close to each other. Therefore, $-\Delta G_{CS} = RT\ ln(k_{CS}/k_{ret}) = 0$, leading to the relation $\Delta E(S_1) = -\Delta G_{CR}$ in the case of HQN. By using this relation and eq 5b together with the values of $\Delta E(S_1)$, E_{ox}, and E_{red} (Table IV) for HQN, ΔG_s in benzene solution has been obtained to be 0.40 eV. With this value of ΔG_s, $-\Delta G_{CR}$ and $-\Delta G_{CS}$ in benzene solutions of the compounds examined here have been evaluated by means of eq 5 and by using the values in Table IV. The free energy gap dependences of the ET rate constants in benzene solutions at room temperature are illustrated in Figure 5. We can see clearly that k_{CS} increases with $-\Delta G_{CS}$, while k_{CR} decreases with $-\Delta G_{CR}$ throughout the energy gap region examined here (0 eV $< -\Delta G_{CS} <$ 1 eV and 1 eV $< -\Delta G_{CR} <$ 2 eV).

Assuming the nonadiabatic mechanism of the ET process, we have examined the experimental results of the energy gap dependence of ET rates given in Table III and Figure 5 by means of eq 2. The solid line in Figure 5 was calculated by using the parameter values of $\lambda_s = 0.18$ eV, $\lambda_v = 0.6$ eV, $\hbar\langle\omega\rangle = 0.15$ eV, and $V = 3.8$ meV, which seems to reproduce the experimental results reasonably well in comparison with the previously reported results obtained by similar analysis of the ET reaction in some other kinds of quinone-linked porphyrin compounds.[16,28] The dotted line in Figure 5 was calculated with $\lambda_s = 0.60$ eV, $\lambda_v =$

(27) (a) Yao, H.; Okada, T.; Mataga, N. *J. Phys. Chem.* **1989**, *93*, 7388. (b) Mataga, N.; Nishikawa, S.; Asahi, T.; Okada, T. *Ibid.* **1990**, *94*, 1443.

(28) (a) Wasielewski, M. R.; Niemczyk, M. P.; Svec, W. A.; Pewitt, E. B. *J. Am. Chem. Soc.* **1985**, *107*, 1080. (b) Harrison, R. J.; Pearce, B.; Beddard, G. S.; Cowan, J. A.; Sanders, J. K. M. *Chem. Phys.* **1987**, *116*, 492.

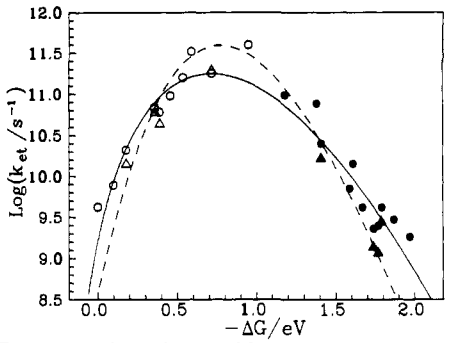

Figure 5. Energy gap dependences of k_{CS} and k_{CR}. O, k_{CS} in benzene; ●, k_{CR} in benzene; △, k_{CS} in toluene; ▲, k_{CR} in toluene. Theoretical curves were calculated by using eq 2 with the following parameter values: —, $\lambda_s = 0.18$ eV, $\lambda_v = 0.6$ eV, $\hbar\langle\omega\rangle = 0.15$ eV, and $V = 3.8$ meV; - - -, $\lambda_s = 0.60$ eV, $\lambda_v = 0.2$ eV, $\hbar\langle\omega\rangle = 0.15$ eV, and $V = 5.0$ meV.

0.2 eV, $\hbar\langle\omega\rangle = 0.15$ eV, and $V = 5.0$ meV, which can hardly reproduce the observed energy gap dependence of the rate constants. Therefore, use of the relatively small λ_s value in eq 2 seems to give better agreements with observed results of the energy gap dependences including both CS and CR reactions. If we use the Marcus equation (eq 6)[29] for the evaluation of λ_s in benzene solution, λ_s is almost 0 because the static (ϵ_s) and optical (ϵ_∞) dielectric constants of benzene liquid are almost equal:

$$\lambda_s = e^2\left(\frac{1}{2r_D} + \frac{1}{2r_A} - \frac{1}{r}\right)\left(\frac{1}{\epsilon_\infty} - \frac{1}{\epsilon_s}\right) \qquad (6)$$

where r_D and r_A are radii of D and A, respectively, and r is the center-to-center distance between D and A. However, the λ_s value which can reproduce the quantitative experimental results of k_{CS} and k_{CR} of the present work is considerably larger than 0. This result suggests the existence of more or less specific solute–solvent interactions in benzene solutions where the simple linear response for the polarization of solvent, assumed to be a dielectric continuum, might be a rather poor approximation. It should be noted here also that this result seems to be consistent with some deviation of fluorescence solvatochromism from the prediction by the linear response of solvent polarization in benzene solutions.[30,31]

At any rate, the present experimental results on the energy gap dependences of k_{CS} and k_{CR} obtained by employing fixed-distance P–Q dyads in benzene solutions at room temperature (22 °C) seem to be reproduced reasonably well by using the approximate formula of eq 2. Nevertheless, we cannot recognize the clear indication of the inverted behavior of k_{CS} even at $-\Delta G_{CS} = 1.0$ eV, while k_{CR} of the P^+–Q^- state shows only the inverted behavior. Further extension of the measurement to the system with larger $-\Delta G_{CS}$ values is necessary for the examination of the inverted effect in the photoinduced CS reaction of this P–Q system. Moreover, although both the energy gap dependences of k_{CS} and k_{CR} at room temperature (22 °C) have been reproduced approximately by the simplified formula of eq 2, simulation of the temperature dependence of these ET rate constants with the approximate formula of eq 2 does not seem to be easy, revealing to some extent the true character of this approximate formula, as discussed later in this paper. Another important problem concerning the energy gap dependence of the ET rate constant is the effect of solvent polarity on it.[2,6] We have also made detailed studies on this problem by using these fixed-distance P–Q dyads, the results of which show deviations from the prediction by the simplified formula of eq 2 and will be discussed later in this paper.

(C) Temperature Dependence of k_{CS} and k_{CR} in Toluene Solutions. We have investigated the temperature dependences

(29) Marcus, R. A. *J. Chem. Phys.* **1956**, *24*, 966.
(30) (a) Lippert, E. *Z. Naturforsch.* **1955**, *109*, 541; (b) *Ber. Bunsen Ges. Phys. Chem.* **1957**, *61*, 962.
(31) Mataga, N.; Kaifu, Y.; Koizumi, M. (a) *Bull. Chem. Soc. Jpn.* **1955**, *28*, 690; (b) **1956**, *29*, 465.

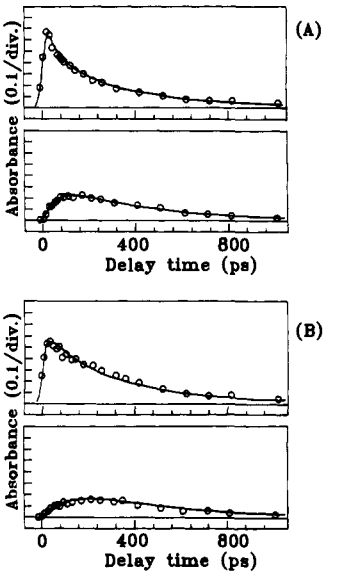

Figure 6. Time profiles of transient absorbance of HQ in toluene observed by excitation with a 532-nm picosecond pulse at 295 (A) and 223 K (B). The wavelengths for the observation were 445 (top) and 700 nm (bottom), respectively. The solid lines are the simulated curves by convolution of exciting pulse, transient absorption (eq 3), and probing pulse, assuming the following values for lifetime of S_1 and IP states: (A) $\tau_s = 65$ ps and $\tau_{ion} = 350$ ps; (B) $\tau_s = 130$ ps and $\tau_{ion} = 350$ ps.

of k_{CS} and k_{CR} in the range from 193 to 295 K in toluene solutions by means of transient absorption spectral measurements. Although we have used toluene instead of benzene as the solvent because the measurements of the transient absorption covering much wider temperature range are possible, time-resolved absorption spectra as well as time profiles of transient absorbance of P–Q systems in toluene solution are very similar to those in benzene solution. Moreover, the energy gap dependences of ET rate constants in toluene solutions are also very similar to those in benzene solutions at room temperature, as indicated in Figure 5.

Time profiles of transient absorbance of HQ in toluene at 295 and 223 K are indicated in Figure 6. By means of the same method for the analysis of the experimental results as in the case of benzene solutions, we have determined the k_{CS} and k_{CR} values of several P–Q systems at various temperatures, results of which are collected in Table V together with the values of the energy gap and the activation energy of the ET reaction. The temperature dependences of k_{CS} and k_{CR} are also plotted against T^{-1} in Figure 7.

We can see clearly that, although k_{CS} shows temperature dependence and its extent increases with a decrease of the reaction exothermicity $-\Delta G_{CS}$, k_{CR} is almost temperature-independent and does not show such a systematic dependence on the free energy gap $-\Delta G_{CR}$ as in the case of k_{CS}. The observed effect of $-\Delta G_{CS}$ upon the temperature dependence of k_{CS} indicates the increase of the activation energy ΔG^* with decrease of $-\Delta G_{CS}$, as actually determined in Table V. This result qualitatively agrees with the classical treatment of Marcus:[29]

$$k_{et} = A\exp(-\Delta G^*/k_B T) \qquad (7)$$

where $\Delta G^* = (\lambda + \Delta G)^2/4\lambda$ and $\lambda = \lambda_s + \lambda_v$. However, the practically activationless ET in the CR reaction for all energy gap regions examined here cannot be interpreted by the classical treatment of Marcus but is almost entirely due to quantum mechanical nuclear tunneling,[20] that is, high-frequency intramolecular vibrational modes play a dominant role in assisting the CR reaction in the region of $-\Delta G_{CR} > 1$ eV.

This difference between the CS and the CR reactions with respect to their temperature dependences might be due to the difference of the observed energy gap region, the normal region

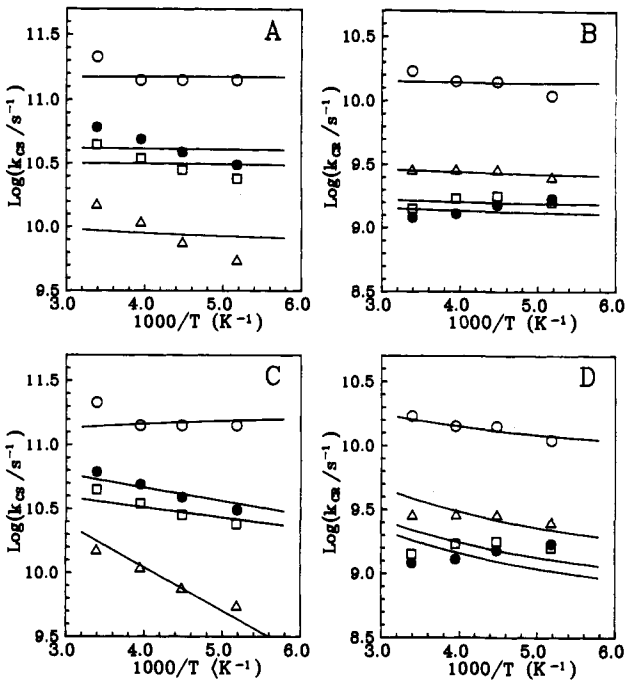

Figure 7. Temperature dependences of k_{CS} (A and C) and k_{CR} (B and D) in toluene solutions in the case of several P–Q systems with different energy gap for ET reactions. ○, ZQC ($-\Delta G_{CS}$ = 0.72 eV; $-\Delta G_{CR}$ = 1.41 eV); □, ZQ2M ($-\Delta G_{CS}$ = 0.39 eV; $-\Delta G_{CR}$ = 1.74 eV); ●, ZQN ($-\Delta G_{CS}$ = 0.36 eV; $-\Delta G_{CR}$ = 1.77 eV); △, HQ ($-\Delta G_{CS}$ = 0.18 eV; $-\Delta G_{CR}$ = 1.79 eV). The solid lines were calculated by using eq 2, with the following parameter values: A, λ_s = 0.18 eV, λ_v = 0.6 eV, $\hbar\langle\omega\rangle$ = 0.15 eV, and V = 3.8, 2.2, 2.7, and 2.4 meV (top to bottom); B, λ_s = 0.18 eV, λ_v = 0.6 eV, $\hbar\langle\omega\rangle$ = 0.15 eV, and V = 2.6, 2.5, 2.5, and 3.8 meV (top to bottom); C, λ_s = 0.60 eV, λ_v = 0.2 eV, $\hbar\langle\omega\rangle$ = 0.15 eV, and V = 3.0, 4.3, 3.1, and 7.1 meV (top to bottom); D, λ_s = 0.60 eV, λ_v = 0.2 eV, $\hbar\langle\omega\rangle$ = 0.15 eV, and V = 4.1, 7.0, 6.6, and 11.3 meV (top to bottom).

Table V. Temperature Dependences of k_{CS} and k_{CR} of Several P–Q Systems and Activation Energies as Well as Energy Gaps for the ET Reactions

		T (K)				ΔG^*	$-\Delta G$
		295	253	223	193	(*kcal/mol*)	(eV)
ZQC	k_{CS} (10^{10} s^{-1})	20	14	14	14	~0	0.72
	k_{CR} (10^9 s^{-1})	17	14	14	12	~0	1.41
ZQ2M	k_{CS} (10^{10} s^{-1})	4.5	3.5	2.8	2.4	0.75	0.39
	k_{CR} (10^9 s^{-1})	1.4	1.7	1.8	1.6	~0	1.74
ZQN	k_{CS} (10^{10} s^{-1})	6.1	4.9	3.9	3.1	0.73	0.36
	k_{CR} (10^9 s^{-1})	1.3	1.3	1.5	1.7	~0	1.77
HQ	k_{CS} (10^{10} s^{-1})	1.5	1.1	0.76	0.55	1.3	0.18
	k_{CR} (10^9 s^{-1})	2.9	2.9	2.9	2.5	~0	1.79

for CS and the inverted region for CR. Namely, the thermal activation may be an important factor in determining the energy gap dependence of the ET reaction in the normal region, but it does not play any such important role in determining the energy gap dependence of the reaction in the inverted region, or in the "large energy gap" ($-\Delta G > \lambda$) region. As stated above, tunneling due to high-frequency intramolecular vibrations seems to play the most important role in promoting the reaction. The energy gap dependence of the reaction in this case may be related to the decrease of the transition probability due to this tunneling with the increase of the $-\Delta G$.

(D) Analyses of the Temperature Dependences and the Energy Gap Dependences of the ET Rate Constants on the Basis of the Simple Theoretical Formula. Only two types of vibrational modes are involved in eq 2, where the low-frequency polarization mode of solvent (~10 cm^{-1}) and the high-frequency intramolecular vibrational mode of D and A molecules (500–3000 cm^{-1}) are denoted by s and v, respectively, and $\hbar\langle\omega\rangle$ is the vibrational quantum with the averaged frequency of the latter. Owing to this approximation, eq 2 is very simple and convenient for comparison with experimental results. Moreover, in spite of such an approximation, eq 2 could reproduce the characteristic feature of the energy gap dependence of the ET rate in benzene and toluene solutions reasonably well as described in section B.

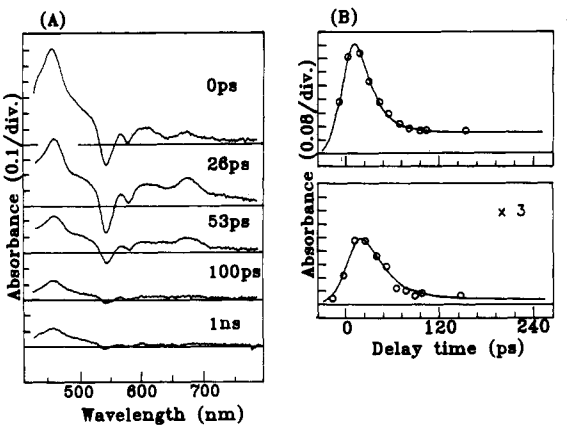

Figure 8. (A) Time-resolved transient absorption spectra of ZQ2M in THF observed by excitation with a 532-nm picosecond pulse. (B) Time profiles of transient absorbance of ZQ2M in THF at 460 (top) and 650 nm (bottom).

Experimental results on the temperature dependences of ET rate constants in toluene solutions of some P–Q systems as described in section C have been analyzed quantitatively by using eq 2, as demonstrated in Figure 7. In this analysis, we assumed that $-\Delta G$, V, λ_s, and λ_v were temperature-independent. The solid lines in Figures 7A and B were calculated by using eq 2, with λ_s = 0.18 eV, λ_v = 0.6 eV, and $\hbar\langle\omega\rangle$ = 0.15 eV, which were the best parameters to reproduce the energy gap dependences of the ET rate constants at room temperature. The temperature dependence of k_{CR} can be reproduced fairly well by these parameters, while that of k_{CS} cannot be reproduced by them.

By assuming that λ_s = 0.60 eV and λ_v = 0.20 eV, the agreement between the calculated and observed temperature dependences of k_{CS} becomes much better, as shown in Figure 7C. However, calculations with these parameters cannot reproduce the temperature dependence of k_{CR}, as indicated in Figure 7D. Moreover, the energy gap dependence of the ET rate constants calculated by eq 2 with these parameters cannot reproduce the observed results, as indicated in Figure 5. These results show that one can hardly find optimum values of the parameters λ_s, λ_v, and $\hbar\langle\omega\rangle$ in eq 2, which can reproduce quantitatively the energy gap dependences and the temperature dependences of k_{CS} and k_{CR} in this P–Q system at the same time. In principle, $-\Delta G$ and λ_s may be temperature-dependent. However, the temperature dependence of the solvation energy in an only weakly polar solvent (toluene) will be very small.

(E) Photoinduced CS and CR of the Intramolecular IP State of Fixed-Distance Porphyrin–Quinone Dyads in Polar Solutions at Room Temperature. As an example of the time-resolved absorption spectra of porphyrin–quinone dyads in polar solutions, picosecond time-resolved spectra and time profiles of transient absorbances of ZQ2M in THF and BuCN solutions are indicated in Figures 8 and 9, respectively. The time-resolved spectra and time profiles of transient absorbance of the same system in benzene are given in Figure 3.

With an increase of solvent polarity, the absorption band due to the porphyrin cation around 670 nm becomes less prominent and more rapidly disappears, which seems to indicate that the CR decay of the intramolecular IP state formed by photoinduced CS becomes much faster with an increase of the solvent polarity while the rate of the photoinduced CS is not much affected by the same increase. We have observed already similar effects of solvent polarity upon the photoinduced CS and CR of the product IP state in the case of the fixed-distance zinc porphyrin–

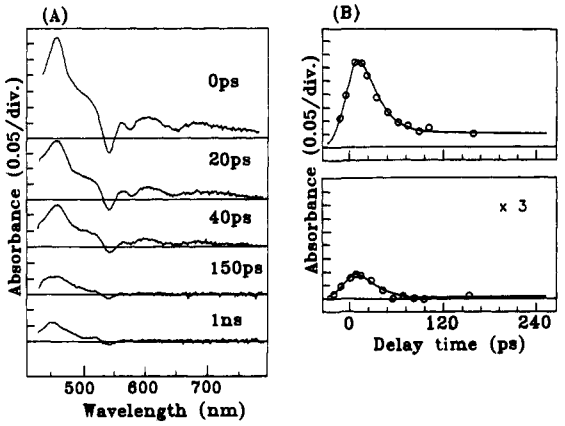

Figure 9. (A) Time-resolved transient absorption spectra of ZQ2M in BuCN observed by excitation with a 532-nm picosecond pulse. (B) Time profiles of transient absorbance of ZQ2M in BuCN at 460 (top) and 650 nm (bottom).

pyromellitimide dyad.[32] These solvent polarity effects upon the ET rate constants can be qualitatively interpreted as follows. In general, with an increase of the solvent polarity, the free energy gap for the CR reaction of the IP state decreases and that for the photoinduced CS reaction increases, while the solvent reorganization energy will increase in both cases according to the conventional ET theories. Moreover, in both of the zinc porphyrin–pyromellitimide and –quinone systems, the photoinduced CS reaction is in the normal region while the CR reaction of the IP state is in the inverted region. Therefore, k_{CS} is not much affected by solvent polarity on the one hand, while k_{CR} shows a rather drastic increase with an increase of the solvent polarity.

The above results of the time-resolved spectral measurements on ZQ2M may be analyzed on the basis of Scheme I and eq 3. By simulation of the time profile of absorbance observed by the picosecond laser photolysis method with the convolution of $A_\lambda(t)$ (eq 3), the excitation pulse, and the probe pulse, the lifetimes of the S_1 and the IP state of ZQ2M in THF have been obtained to be $\tau_s = 12$ ps and $\tau_{ion} = 23$ ps, from which the rate constants have been evaluated as follows: $k_{CS} = \tau_s^{-1} - \tau_0^{-1} = 8.3 \times 10^{10}$ s^{-1} and $k_{CR} = \tau_{ion}^{-1} = 4.3 \times 10^{10}$ s^{-1}. As in the case of the benzene solutions, the ϵ values used in the above simulation have been determined by means of measurements of transient absorbance and ground-state bleaching as well as their excitation intensity dependences. The ϵ values in THF solution for ZnP–Q systems are indicated in Table II. For the relatively slow ET processes, values of τ_s and τ_{ion} have been evaluated directly from the decay curves in the observed time profiles of the transient absorbance. We have evaluated τ_s values also by the fluorescence decay curve measurements. The k_{CS} value determined from the fluorescence lifetime measurement was in agreement with that obtained from the transient absorbance measurement.

In the case of the BuCN solution of ZQ2M, the decay times of absorbance at various wavelengths were all equal to 20 ps. This result indicates that, because $\tau_s > \tau_{ion}$ in BuCN solution due to the mechanism discussed in the beginning of this section, the absorbance decay time is equal to τ_s also at the wavelength of the ion absorption, since the rise and decay times of the IP state are given by eq 8 according to Scheme I:

$$[P^+–Q^-] = \{A_0\Phi_{ET}\tau_s^{-1}/(\tau_s^{-1} - \tau_{ion}^{-1})\}\{\exp(-t/\tau_{ion}) - \exp(-t/\tau_s)\} \quad (8)$$

In order to obtain the τ_{ion} value, we must evaluate the rise time of the ion absorption at 650 nm. However, such an evaluation is very difficult due to the condition $\tau_s > \tau_{ion}$, as indicated by the transient spectra and absorbance time profile in Figure 9. The

(32) Osuka, A.; Nakajima, S.; Maruyama, K.; Mataga, N.; Asahi, T. *Chem. Lett.* **1991**, 1003.

Table VI. τ_s, τ_{ion}, k_{CS}, and k_{CR} Values of ZQ2M in Benzene, THF, and BuCN Solutions

solvent	τ_s (ps)	k_{CS} (10^{10} s^{-1})	τ_{ion} (ps)	k_{CR} (10^{10} s^{-1})
benzene	16	6.0	440	0.23
THF	12	8.3	23	4.3
BuCN	20	4.9	<20	>5.0

Table VII. τ_s, τ_{ion}, k_{CS}, and k_{CR} Values of ZQ3C in Benzene, THF, and BuCN Solutions

solvent	τ_s (ps)	k_{CS} (10^{11} s^{-1})	τ_{ion} (ps)	k_{CR} (10^{11} s^{-1})
benzene	2.5	4.0	10.3	0.97
THF	1.8	5.5	5.2	1.9
BuCN	1.9	5.3	5.9	1.7

τ_s, τ_{ion}, and k_{CS} as well as k_{CR} values of ZQ2M in THF and BuCN are collected in Table VI together with those in benzene solution in order to compare the solvent polarity effect on the photoinduced CS with that on the CR of the product IP state.

We have measured very fast ET processes as in the case of the ZQ3C by means of the femtosecond laser photolysis method. Results of measurements on ZQ3C in THF and BuCN are indicated in Table VII together with those in benzene. In this case, the effect of the solvent polarity on k_{CR} is much smaller compared to the case of ZQ2M. The results of the measurements on the energy gap dependence of k_{CR} of these P–Q dyads in benzene solution as given in Table III and Figure 5 indicate that, although k_{CR} of ZQ3C is in the inverted region, it is rather close to the top region, which seems to make the solvent polarity effect on k_{CR} relatively small.

We have examined also the solvent polarity effects on the photoinduced CS and CR of the IP state of H_2P–Q dyads. Our results on these systems have indicated that although $\tau_s < \tau_{ion}$ in benzene solutions $\tau_s \geq \tau_{ion}$ in THF solutions. The oxidation potential of H_2P is 0.2 eV higher than that of ZnP, and the energy of the 0–0 band of S_1–S_0 transition of H_2P is 0.15 eV lower than that of ZnP. This makes the energy gap of the photoinduced CS of H_2P–Q much smaller than that of ZnP–Q, with the same quinone group leading to much smaller k_{CS} values of the H_2P–Q system, which causes rather easily the condition $\tau_s \geq \tau_{ion}$ in polar solutions. This condition may certainly hold also in BuCN, but its confirmation by transient absorption spectral measurements was not possible due to the very small solubility of H_2P–Q compounds in BuCN.

Accordingly, an accurate determination of the k_{CS} value was possible for almost all compounds studied here either by means of measurements of both transient absorption spectra and fluorescence lifetimes or only by the fluorescence lifetime measurements in both THF and BuCN solutions. However, accurate determination of the k_{CR} value in polar solutions was possible only for the limited number of ZnP–Q compounds in THF solutions.

In section A, we discussed the possible effects of hindered rotations around the phenyl-CH_2 and/or CH_2-quinone single bonds, leading to the rotational-angle-dependent ET or the formation of rotational conformers with different ET rates. In benzene and toluene solutions, observed decay curves of $P^*(S_1)$–Q and P^+–Q^- states were not multiexponential or nonexponential but single exponential, which suggested that the CS and CR rates in these dyads in benzene and toluene solutions were not affected appreciably by internal rotations. As described above, the decay curves of fluorescence and transient absorption observed in THF and BuCN solutions are also single exponential. Therefore, no special effect of internal rotation on the ET process caused by the change of solvent polarity can be recognized.

(F) Effects of Solvent Polarity on the Free Energy Gap Dependence of Photoinduced CS Rate Constant. In order to discuss the solvent polarity effect on the energy gap dependence of the ET rate constant of these fixed-distance dyads, we have evaluated $-\Delta G_{CS}$ and $-\Delta G_{CR}$ in THF and BuCN solutions by the conven-

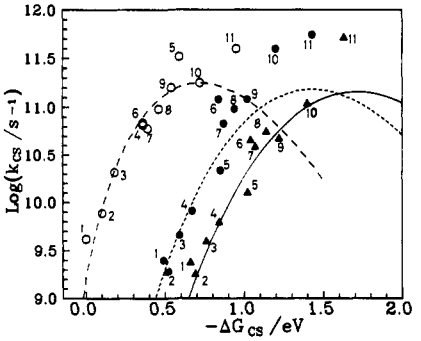

Figure 10. Solvent effect on the energy gap dependence of k_{CS}. Observed values: ○ (in benzene), 1, HQN, 2, HQ1M, 3, HQ, 4, HQC, 5, HQ3C, 6, ZQN, 7, ZQ2M, 8, ZQ1M, 9, ZQ, 10, ZQC, and 11, ZQ3C; ● (in THF) and ▲ (in BuCN), 1, HQN, 2, HQ2M, 3, HQ1M, 4, HQ, 5, HQC, 6, ZQN, 7, ZQ2M, 8, ZQ1M, 9, ZQ, 10, ZQC, and 11, ZQ3C. Lines are calculated by using eq 2 with common parameters $V = 3.8$ meV, $\lambda_v = 0.6$ eV, $\hbar\langle\omega\rangle = 0.15$ eV, and $\lambda_s = 0.18$ eV in benzene, 0.87 eV in THF, and 1.15 eV in BuCN.

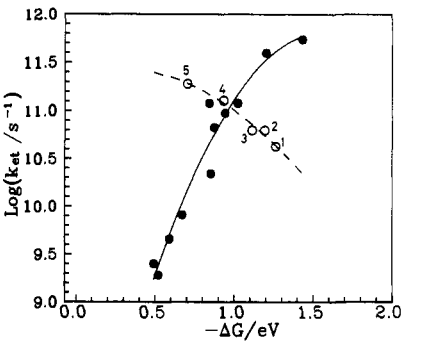

Figure 11. Energy gap dependences of k_{CR} (○) and k_{CS} (●) in THF solution. Broken and solid lines are just to guide eye. ○, 1, ZQ2M, 2, ZQ1M, 3, ZQ, 4, ZQC, and 5, ZQ3C. For the numbering and compounds of k_{CS}, see Figure 10.

tional method, using the values of E_{ox}, E_{red}, and $\Delta E(S_1)$ given in Table IV and eqs 5a, 5b, and 9:

$$\Delta G_s = e^2\left(\frac{1}{2r_D} + \frac{1}{2r_A}\right)\left(\frac{1}{\epsilon_s} - \frac{1}{\epsilon_r}\right) - \frac{e^2}{\epsilon_s r} \qquad (9)$$

where r is the center-to-center distance between porphyrin and quinone chromophores, r_D and r_A are effective radii of the porphyrin cation and the quinone anion, taken to be 5 Å and 3.5 Å, respectively, and ϵ_r is the dielectric constant of solvent in which E_{ox} and E_{red} have been determined.

It should be noted here that we have estimated the value of ΔG_s in eq 5b by using only the experimental data without resorting to any correction formula in the case of benzene solutions. We have adopted this procedure for the benzene solution because the apparent polarity of benzene seems to be different from the estimation based on the bulk dielectric constant due to its specific interactions with polar or ionic solutes. However, for the more polar solvents like THF and BuCN, many previous studies[1,2,7,9,10,15,16,28a,33] seem to indicate that the procedures as used in eqs 5 and 9 are not very bad approximations and give reasonable results in many cases.

The k_{CS} values in THF and BuCN solution determined in this work as described in section E are plotted against $-\Delta G_{CS}$ in Figure 10 together with those in benzene solution for comparison. The k_{CS} vs $-\Delta G_{CS}$ relations in three kinds of solvent with different polarities as indicated in Figure 10 are all in the normal region. The k_{CS} vs $-\Delta G_{CS}$ relation shifts to the side of the larger energy gap with increase of the solvent polarity. This result is qualitatively in accordance with the prediction of conventional ET theories.

We have tried to reproduce these results of the energy gap dependence of CS rate constants by eq 2. The lines in Figure 10 are simulations of the observed results with eq 2, where $V = 3.8$ meV, $\lambda_v = 0.6$ eV, and $\hbar\langle\omega\rangle = 0.15$ eV are fixed and only λ_s is varied depending on solvent polarity, i.e., $\lambda_s = 0.18$ eV in benzene, $\lambda_s = 0.87$ eV in THF, and $\lambda_s = 1.15$ eV in BuCN.

These calculations using eq 2 appear to reproduce reasonably well the observed results and seem to give the best fit to each series of data in the normal region. It should be noted here that Joran et al.[33] and Wasielewsiki et al.[16b,c] reported also more or less similar shifts of the k_{CS} vs $-\Delta G_{CS}$ curves of fixed-distance P–Q systems in the normal region to the side of the larger energy gap with increase of solvent polarity. Nevertheless, the discrepancy between calculated and observed results increases near the top region in all case. Namely, the observed results do not show the indication of the inverted behavior even at the largest value of the energy gaps examined in this work, while the results of the calculation fitted to the normal region show clearly the inverted behaviors in all cases at those large values of the energy gap. One of the possible mechanisms to interpret the lack of the inverted region in the observed results of the photoinduced CS seems to be the participation of the electronic excited states of the IP in the course of the ET.[7,11] We have examined this possibility in the case of the porphyrin–quinone systems on the basis of the known energy levels of relevant radical ions, results of which show, however, that such a possibility is negligible in the present systems. Further theoretical and experimental examinations seem to be necessary.

(G) Comparison of the Solvent Effect on the Energy Gap Dependence of k_{CR} with That of k_{CS}. As described in section E, the experimental measurement of the energy gap dependence of k_{CR} in polar solvents is rather difficult. Because k_{CS} is in the normal region in most cases, it shows little change with increase of solvent polarity owing to the simultaneous increase of the energy gap, $-\Delta G_{CS}$, and the solvent reorganization energy. On the other hand, k_{CR} of the IP state produced by photoinduced CS will be in the inverted region in most cases. Therefore, it shows a large increase with increase of solvent polarity due to the decrease of the energy gap, $-\Delta G_{CR}$, and, probably, the increase of the solvent reorganization energy. These factors can easily realize the condition $k_{CS} < k_{CR}$ in polar solvent, which makes difficult the systematic studies of the solvent polarity effect on the energy gap dependences of k_{CR}. Moreover, the usual ET theories predict that the energy gap dependence of the ET rate constant and the solvent effect on it will be essentially similar in both the photoinduced CS reaction and the CR reaction of product IP state.

The above described circumstances might have led to the result that there has been almost no clear-cut experimental confirmation of this problem up to now. Nevertheless, it seems to be necessary and important to examine this problem by using the fixed-distance D–A systems in various solvents of different polarities, because the above theoretical expectation will not be realized if there exists any essential difference of ET mechanism between CS and CR reactions or between the normal and inverted regions. Although the energy gap range where we have measured the k_{CR} values is rather limited owing to the above described circumstances, we could have determined accurately several k_{CR} values near the top region.

In Figure 11, k_{CR} values are plotted together with k_{CS} values against $-\Delta G$ in the case of THF solution, where the k_{CR} vs $-\Delta G_{CR}$ curve crosses with the k_{CS} vs $-\Delta G_{CS}$ curve. This result indicates that the reorganization energy for the CR of the intramolecular IP state is considerably smaller than that of the photoinduced CS in THF solution. It should be noted here that we could not observe such crossing for the same P–Q dyad systems in less polar solvent benzene. Therefore, this crossing between the two curves or the difference between the reorganization energy of CR of the IP state and that of the photoinduced CS seems to be caused by the

(33) Joran, A. D.; Leland, B. A.; Felker, P. M.; Zewail, A. H.; Hopfield, J. J.; Dervan, P. B. *Nature (London)* **1987**, *327*, 508.

interactions between the solute chromophores undergoing ET and the polar solvent surrounding them.

One of the possible mechanisms for this crossing seems to be related to remarkable difference between the temperature dependences of k_{CS} (in the normal region) and k_{CR} (in the inverted region) observed in toluene solutions. Namely, the solvent reorganization and the thermal activation play important roles in regulating the CS reaction, while the reorganization and quantum mechanical tunneling associated with the intramolecular vibrations are of crucial importance for the CR reaction. With the increase of the solvent polarity, the contribution of the solvent reorganization energy to the reaction rate will increase in general. Nevertheless, in view of the predominant importance of the intramolecular vibrations and quantum mechanical tunneling in the inverted region, the energy gap dependence of the CR reaction might not be affected so much as that of the CS reaction by the increase of solvent polarity. If this is the case, although the k_{CS} vs $-\Delta G_{CS}$ curve shifts considerably to the larger energy gap side in THF compared to benzene solution, the k_{CR} vs $-\Delta G_{CR}$ curve will be close to that in benzene solution as it is actually observed in the present system. It should be noted here that a somewhat similar tendency concerning the difference between the solvent polarity effect on the energy gap dependence of photoinduced ET in the normal region and that of back-ET in the inverted region has been reported recently[34] in the case of the intramolecular ET of a quite different system of donor-substituted Re(I) complexes in polar solutions where also the effect of the high-frequency quantum modes seems to be predominant in the back-ET.

Another possible mechanism is the existence of nonlinear or some specific interactions between the solute IP and surrounding polar solvent in the course of the ET process. Namely, when the nonlinear response in the interaction of the IP state with polar solvent is appreciable, the energy gap dependences and solvent reorganization energy of CS and CR reactions are different from each other.[12,35] In this case, the free energy curvature around the minimum of the IP state is larger than that of the neutral state,[12,35] which leads to the larger λ_s in CS than in CR, just as some model calculations have demonstrated.[35]

(H) Concluding Remarks. In this study, we have examined the energy gap dependences of photoinduced CS and CR of the product IP state of D–A systems in nonpolar or only weakly polar solvent as well as in moderately and strongly polar solutions by means of picosecond–femtosecond laser photolysis studies upon the series of fixed-distance porphyrin–quinone dyads in order to avoid the ambiguities caused by the change of D–A distance in the course of ET reaction of unlinked systems or D–A systems linked by spacers with large flexibility. Moreover, we have examined also the temperature effects on the photoinduced CS and CR of IP of these dyads in nonpolar media in order to get different kinds of information on these processes.

The observed k_{CS} vs $-\Delta G_{CS}$ relations have demonstrated that they are in the normal region up to the neighborhood of the top region. Those k_{CS} vs $-\Delta G_{CS}$ relations at room temperature can be reproduced fairly well by semiclassical formula taking into consideration the high-frequency quantum mode of intramolecular vibration approximated by a single averaged mode in both nonpolar and polar solutions and by increasing λ_s with increase of the solvent polarity, keeping other parameter values constant, at relatively small $-\Delta G_{CS}$ values in the normal region. However, the discrepancy between the observed and calculated results becomes large at large $-\Delta G_{CS}$ values near the top region, where the observed results do not show the inverted behavior and the participation of the excited electronic state of IP to the CS is not possible on the basis of the observed spectra of ion radicals, while calculated results show the inverted behavior.

On the other hand, the observed k_{CR} vs $-\Delta G_{CR}$ relations of these dyads have been confirmed to be in the inverted region. The results in benzene and toluene solutions at room temperature can be approximately reproduced by the same semiclassical formula with the same parameter values as used for the CS reaction. However, the investigation on the temperature dependence of k_{CS} and k_{CR} in toluene solutions has revealed that the activation energy for CS increases with a decrease of $-\Delta G_{CS}$ while CR of IP is activationless at all $-\Delta G_{CR}$ values examined, which indicates the dominant effect of the quantum mechanical tunneling due to the high frequency nodes for ET in the inverted region. Namely, we cannot reproduce the temperature dependences of CS and CR by using the same λ values in the formula.

We have also made a systematic study of the solvent polarity effect on the energy gap dependence of k_{CR} of the IP state by employing the same series of the fixed-distance dyads and comparing it with that of k_{CS}. The results in THF solutions have demonstrated the crossing of the k_{CR} vs $-\Delta G_{CR}$ curve with the k_{CS} vs $-\Delta G_{CS}$ curve, indicating that the reorganization energy of the CR reaction is considerably smaller than that of the CS reaction of the same system, while such crossing was not observed in benzene solution of the same system. This means that although the k_{CS} vs $-\Delta G_{CS}$ curve shifted considerably to the side of larger $-\Delta G_{CS}$ in THF compared with that in benzene solution, the k_{CR} vs $-\Delta G_{CR}$ curve does not show such a shift, and actually the k_{CR} vs $-\Delta G_{CR}$ curve in THF approximately coincides with that in benzene solution. The different energy gap dependence and the different reorganization energy between the CS and CR reaction of the same fixed-distance dyad systems in the same solvent THF do not seem to be in accordance with the prediction by the conventional ET theories. These results seem to be related to the remarkable difference between the temperature dependences of k_{CS} (in the normal region) and k_{CR} (in the inverted region) and may be ascribed to the dominant effect of intramolecular high-frequency vibrations and quantum mechanical tunneling for the ET process in the inverted region leading to the small effect of the solvent reorganization in spite of the increase of solvent polarity. It should be noted here that these quite remarkable differences between the CS and the CR reactions seem to be inherent in the fundamental difference between the ET mechanisms in the normal and inverted regions. In the inverted region, the ET takes place by the transition between different eigenstates of the same Hamiltonian due to the coupling with promoting and accepting quantum modes of the intramolecular vibrations. Such vibrational overlap plays a far more important role in regulating ET in the inverted region than in the normal region due to the embedded nature of the potential energy surfaces of initial and final states, which is the same circumstance as in the case of the weak coupling limit in the radiationless transition.[36,37] In addition to this, there is another possible mechanism of the nonlinear interactions between the solute IP and the surrounding polar solvent leading to the larger λ in CS than in CR.

Acknowledgment. We are grateful to Dr. T. Odada and Dr. H. Miyasaka for their advice in the experimental measurements. The present work was partially supported by a Grant-in-Aid for Specially Promoted Research (No. 02102005) from the Ministry of Education, Science and Culture of Japan to K.M. and also partially supported by a Grant-in-Aid for Specially Promoted Research (No. 6265006) from the Ministry of Education, Science and Culture of Japan to N.M.

(34) MacQueen, D. B.; Schanze, K. S. *J. Am. Chem. Soc.* **1991**, *113*, 7470.
(35) (a) Enomoto, Y.; Kakitani, T.; Yoshimori, A.; Hatano, Y.; Saito, M. *Chem. Phys. Lett.* **1991**, *178*, 235. (b) Enomoto, Y.; Kakitani, T.; Yoshimori, A.; Hatano, Y. *Chem. Phys. Lett.* **1991**, *186*, 366.
(36) (a) Englman, R.; Jortner, J. *Mol. Phys.* **1970**, *18*, 145. (b) Freed, K. J.; Jortner, J. *J. Chem. Phys.* **1970**, *52*, 6272.
(37) (a) Chen, P.; Duesing, R.; Tapolsky, G.; Meyer, T. J. *J. Am. Chem. Soc.* **1989**, *111*, 8305. (b) Meyer, J. T. *Prog. Inorg. Chem.* **1983**, *30*, 389. (c) Chen, P.; Duesing, R.; Graff, D. K.; Meyer, T. J. *J. Phys. Chem.* **1991**, *95*, 5850.